

# Genetic Factors Regulating Lung Vasculature and Immune Cell Functions Associate with Resistance to Pneumococcal Infection

Magda S. Jonczyk<sup>1</sup>, Michelle Simon<sup>2</sup>, Saumya Kumar<sup>2</sup>, Vitor E. Fernandes<sup>1</sup>, Nicolas Sylvius<sup>3</sup>, Ann-Marie Mallon<sup>2</sup>, Paul Denny<sup>2</sup>, Peter W. Andrew<sup>1\*</sup>

**1** Department of Infection Immunity and Inflammation, University of Leicester, Leicester, United Kingdom, **2** MRC Harwell, Mammalian Genetics Unit, Oxford, United Kingdom, **3** Department of Genetics, University of Leicester, Leicester, United Kingdom

## Abstract

*Streptococcus pneumoniae* is an important human pathogen responsible for high mortality and morbidity worldwide. The susceptibility to pneumococcal infections is controlled by as yet unknown genetic factors. To elucidate these factors could help to develop new medical treatments and tools to identify those most at risk. In recent years genome wide association studies (GWAS) in mice and humans have proved successful in identification of causal genes involved in many complex diseases for example diabetes, systemic lupus or cholesterol metabolism. In this study a GWAS approach was used to map genetic loci associated with susceptibility to pneumococcal infection in 26 inbred mouse strains. As a result four candidate QTLs were identified on chromosomes 7, 13, 18 and 19. Interestingly, the QTL on chromosome 7 was located within *S. pneumoniae* resistance QTL (*Spir1*) identified previously in a linkage study of BALB/cOlaHsd and CBA/CaOlaHsd F2 intercrosses. We showed that only a limited number of genes encoded within the QTLs carried phenotype-associated polymorphisms (22 genes out of several hundred located within the QTLs). These candidate genes are known to regulate TGF $\beta$  signalling, smooth muscle and immune cells functions. Interestingly, our pulmonary histopathology and gene expression data demonstrated, lung vasculature plays an important role in resistance to pneumococcal infection. Therefore we concluded that the cumulative effect of these candidate genes on vasculature and immune cells functions as contributory factors in the observed differences in susceptibility to pneumococcal infection. We also propose that TGF $\beta$ -mediated regulation of fibroblast differentiation plays an important role in development of invasive pneumococcal disease. Gene expression data submitted to the NCBI Gene Expression Omnibus Accession No: GSE49533 SNP data submitted to NCBI dbSNP Short Genetic Variation [http://www.ncbi.nlm.nih.gov/projects/SNP/snp\\_viewTable.cgi?handle=MUS\\_PNEUMONIA](http://www.ncbi.nlm.nih.gov/projects/SNP/snp_viewTable.cgi?handle=MUS_PNEUMONIA).

**Citation:** Jonczyk MS, Simon M, Kumar S, Fernandes VE, Sylvius N, et al. (2014) Genetic Factors Regulating Lung Vasculature and Immune Cell Functions Associate with Resistance to Pneumococcal Infection. PLoS ONE 9(3): e89831. doi:10.1371/journal.pone.0089831

**Editor:** Bernard Beall, Centers for Disease Control & Prevention, United States of America

**Received:** August 18, 2013; **Accepted:** January 27, 2014; **Published:** March 3, 2014

**Copyright:** © 2014 Jonczyk et al. This is an open-access article distributed under the terms of the Creative Commons Attribution License, which permits unrestricted use, distribution, and reproduction in any medium, provided the original author and source are credited.

**Funding:** This work was supported by the European Union-funded Pneumopath Project HEALTH-F3-2009-222983. The funders had no role in study design, data collection and analysis, decision to publish, or preparation of the manuscript.

**Competing Interests:** The authors have declared that no competing interests exist.

\* E-mail: pwa@le.ac.uk

‡ Current address: Gene Effects, Farnham Common, Buckinghamshire, United Kingdom

## Introduction

*Streptococcus pneumoniae* is an important pathogen of humans. It is estimated that pneumococcal diseases cause 5–35% mortality worldwide while less severe pneumococcal infections give rise to high costs of healthcare [1,2]. Numerous reports show that infection, even with a highly virulent pneumococcal strain, may not result in death or severe clinical outcome in all infected individuals [3,4,5,6,7]. This observation suggests there is a genetic component to host susceptibility. However, although the pathogenesis of pneumococcal disease and determinants of pneumococcal virulence are quite well described [8,9,10,11,12,13,14,15], little is known about the genetic aspects of host susceptibility. Identification of the host factors important in resistance or susceptibility to pneumococci could help develop new biomarkers, find novel drug targets and improve our knowledge about the disease and recovery.

Attempts to characterize the genetic factors in pneumococcal pneumonia susceptibility in humans have predominantly taken a candidate gene approach and been limited to a small number of pneumonia cases [16,17,18,19,20]. Unfortunately, the candidate gene approach precludes identification of new genes involved in the disease. Furthermore, while studying a human population a range of factors other than host genetic background can affect the power of disease associations. For example, misdiagnosis of the cases, as well as a number of confounding factors affecting the phenotype, such as previous exposures, lifestyle or medical treatment, can significantly increase noise in the data.

An alternative approach is to use mouse models of pneumococcal diseases. Presently, most of the data on host susceptibility in mice come from comparative studies of pairs of mouse strains representing opposite disease phenotypes (e.g.: resistant and susceptible as measured by animal survival). Such studies have focused on immune cell profiles and inflammatory responses

(predominantly in lungs) at different stages of the disease [3,6,8,9,21,22]. Although these studies delivered much useful information, they have no power to explain what genetic components are responsible for observed phenotypic differences.

Previously we undertook mapping of the disease susceptibility loci using BALB/c and CBA/Ca crosses and a *S. pneumoniae* infection resistance QTL 1 (*Spir1*) was identified on proximal chromosome 7 [23]. The locus spans a 7cM region encompassing too many genes to easily hypothesise a candidate.

A huge drawback in linkage analysis is its low mapping resolution that rarely leads to gene discovery. Additionally, a genetic effect of the QTL may be attributed to the combined effect of several physically linked genetic elements and can be disrupted during an attempt to narrow the QTL [24,25,26,27,28]. Therefore, linkage analysis can benefit hugely from Genome Wide Association studies (GWAS), which attains high mapping resolution [29,30]. Recently GWAS studies in humans proved to be very successful in identification of causal genes involved in common diseases such as diabetes, HDL- and LDL-cholesterol regulation, systemic lupus or Crohn disease [31]. Nevertheless, the GWAS in humans remain very expensive, require tens of thousands of subjects and a huge bioinformatics effort [32]. In comparison, studies in mice can successfully identify disease associations using a fraction of these resources [24,27]. They are also highly reproducible and benefit from availability of excellent mouse models for further functional characterisation of candidate genes [24,33,34].

Currently the Jackson Laboratory (JAX) holds the largest repository of mouse strains (JAX-mouse strains). It offers a wide range of inbred, mutant and genetically engineered mouse strains for which the dense genotyping data and other relevant information are freely available. Recently 17 of the inbred mouse strains from the Jackson Laboratory have been fully sequenced by the Sanger Institute [35]. All these advances in mouse genetics make the mouse increasingly attractive for the genetic dissection of complex traits.

In this study a panel of inbred JAX-mouse strains was evaluated for their susceptibility to infection with pneumococci. Collected phenotype data were then analysed by Efficient Mixed Model Association (EMMA) and Haplotype Association Mapping (HAM) to identify susceptibility loci. The complete sequences within the identified disease QTLs were then examined to narrow the number of candidate genes to those carrying the phenotype-specific polymorphism. Comparative analysis of the pulmonary gene expression in resistant and susceptible mouse strains was also used to support hypotheses of candidate genes and pathways. This approach identified three putative novel susceptibility QTLs, significantly narrowed the previously identified *Spir1* locus [23] and selected a small number of gene candidates for further hypotheses.

Our results indicate an important role of lung vasculature remodelling and immune cell regulation in the resistance to pneumococcal infection. We demonstrated that a prominent feature associated with the resistance was lung perivascular area free from cellular infiltrates. Subsequently we discussed the possible role of lung fibroblasts and/or smooth muscle cells in the resistance to pneumococcal infections. We also hypothesize a role of candidate genes in regulation of the TGF $\beta$  pathway and the vascular and immune cell functions in relation to the resistance to pneumococcal infection.

## Results

### Differences in susceptibility to pneumococcal infection in inbred mouse strains

Variation in susceptibility to pneumococcal infection was examined in 26 inbred JAX-mouse strains and the two Harlan strains, BALB/cOlaHsd and CBA/CaOlaHsd previously used in a linkage study of *S. pneumoniae* susceptibility [23]. Mice were infected intranasally with *S. pneumoniae* strain D39 and observed for 168 h (7 days), after which time each mouse that was alive was considered to have survived the infection. The shortest survival time was 21 h (LP/J) and the longest (for non-survivors) was 154 h (A/J) and the average survival time (excluding survivors) was 49 h. 32% of all tested animals survived infection but among the tested mouse strains the survival rate ranged from 100% to 0%. Survival differed significantly ( $p < 0.001$ ) between the mouse strains as measured by the time (hours) animal survived post-infection (Table 1). The susceptible mouse strains differed significantly in their survival from the resistant strains ( $p < 0.0001$ ) and there was a group of mouse strains, classified as intermediate, that differed from none of the tested strains or only from the strains representing the most extreme phenotype within the resistant or susceptible group of mice ( $p$ -value between 0.05–0.01). The resistant strains had a survival rate of 70%–100%, the susceptible 0%–20%, and the intermediate 30%–50%, (Table 1).

The bacterial load in tissues at the time of death was highly correlated with the survival time (h) with Pearson  $R^2 = 0.83$  and  $R^2 = 0.87$  for bacterial counts in lung and blood respectively. The level of bacteraemia at 24 h post-infection showed a lower correlation with the survival, with  $R^2 = 0.7$ . Interestingly, we found that the intermediate strain, C58/J, with a 50% survival rate, had a very high bacterial load in the lungs at the time of death and all survivors had bacteria present in their lungs at the end of the experiment (Fig. 1C). Furthermore, the susceptible strain, SEA/GnJ, showed low bacterial counts in the blood at 24 h post infection, but nevertheless all animals died in less than 3 days. In contrast, the intermediate strains, DBA/1J and DBA/2J, despite the high 24 h bacteraemia survived on average 84 h and 94 h respectively, and had a 30%–40% survival rate (Fig. 1A, Table 1).

### Genetic susceptibility to *S. pneumoniae* infection is associated with mouse chromosomes 7, 13, 18 and 19

The survival time of the 26 inbred JAX-mouse strains were used to map candidate pneumonia susceptibility loci using two statistical approaches: the Efficient Mixed Model Associations (EMMA) and the Haplotype Association Mapping (HAM). The EMMA mapping was done using the EMMA server and the HAM mapping was done using PLINK software. Two SNP panels (132K and 4Mil) and data for individual mouse were used in the EMMA mapping. The P value was calculated for each SNP in the panels and the SNPs with a P value below  $5 \times 10^{-8}$  were considered significant. For the HAM model the 132K SNP panel and the average survival time were used and the P value cut-off for an inferred haplotype was  $10^{-5}$ . The QTL interval was defined as a region containing SNPs or haplotypes that passed the significance threshold plus 1 Mb upstream or downstream of this region.

Despite conceptual differences of the two methods, the results obtained with each were very similar (Table 2). The QTLs that passed the significance threshold in both mapping methods were selected for further analysis. Consequently four QTLs, on chromosomes 7, 13, 18 and 19, were identified. Interestingly the QTL on chromosome 7 identified in the GWAS approach was located within the previously reported *S. pneumoniae* infection

**Table 1.** Survival of tested inbred mouse strains and disease phenotype after intranasal infection with *S. pneumoniae*, D39.

Mouse strain	Mean survival (h)	SE	Survival rate (%)	Group
LP/J	31	3.4	0	susceptible
C3H/HeJ	31	3.7	0	susceptible
NZW/LacJ	40	1.9	0	susceptible
CBA/CaOlaHsd	46	13.7	10	susceptible
129S1/SvImJ	52	13.1	10	susceptible
CBA/J	54	4.1	0	susceptible
SJL/J	54	13.0	10	susceptible
SEA/GnJ	56	4.0	0	susceptible
BTBRT+ tf/J	59	11.7	0	susceptible
I/LnJ	59	4.9	0	susceptible
SM/J	69	17.5	20	susceptible
PL/J	75	16.1	20	susceptible
NOD/ShiLtJ	77	16.5	30	intermediate
C57BLKS/J	81	21.9	30	intermediate
DBA/1J	84	18.8	30	intermediate
C57L/J	87	17.8	30	intermediate
AKR/J	91	21.1	40	intermediate
DBA/2J	94	20.3	40	intermediate
C57BL/6J	95	20.0	40	intermediate
MA/MyJ	104	21.3	50	intermediate
C57BL/10J	116	18.7	50	intermediate
C58/J	119	16.9	50	intermediate
A/J	140	17.4	70	resistant
FVB/NJ	154	9.2	80	resistant
BALB/cJ	155	12.6	90	resistant
C57BR/cdJ	157	11.3	90	resistant
BALB/cOlaHsd	161	6.7	90	resistant
BALB/cByJ	168	0.0	100	resistant

SE – standard error.

doi:10.1371/journal.pone.0089831.t001

resistance 1 QTL (*Spir1*) identified during linkage analysis of progeny of crosses between CBA/CaOlaHsd and BALB/cOlaHsd [23]. The *Spir1* locus spans 7 cM and the GWAS analysis helped narrow this locus from 13 Mb (24 Mb–37 Mb) to 2.6 Mb (28.7 Mb–31.3 Mb).

### The phenotype-associated SNPs were detected within 22 genes and intergenic regions

The SNPs that passed the genome-wide significance threshold ( $p < 5 \times 10^{-8}$ ) in the EMMA mapping, using the 4Mil SNP panel, were then extracted and the nucleotide variant at the selected SNP position was examined in the tested panel of 26 inbred JAX-mouse strains and in the two Harlan strains (CBA/CaOlaHsd and BALB/cOlaHsd). There were 17 significant SNPs within the QTL on chromosome 7, seven of them within coding sequences for *Ryr1*, *RasGRP4* and *Spint2* and two SNPs within regions annotated as regulatory by the Mouse Phenome Database (Table S1). Four significant SNPs were located within the QTL on chromosomes 13 (within *Ntrk2* gene) and five significant SNPs within the QTL on chromosome 18 (intergenic, upstream of *Smad4* gene) (Table S1).

The QTL on chromosome 19 had the highest number of significant SNPs, 169, including 79 SNPs located within five proteins: *Stambpl1*, *Acta2*, *Fas*, *Slc16a12* and *Kif20b* (Table S1).

Comparison of the significant SNP variants between the tested mouse strains showed a clear separation of the resistant strains from the others (Table S1), although at some of the positions within the QTLs on chromosomes 18 and 19 a few intermediate mouse strains displayed a SNP variant associated with resistance (for example, C58/J, MA/MyJ and NOD/ShiLtJ within chromosome 18 and C57BLKS/J, C57L/J and C58/J within QTL on chromosome 19). Furthermore, in case of two resistant strains: A/J and C57BR/cdJ some of the SNPs within the QTL on chromosome 7 displayed a susceptible variant. The later strain also displayed a susceptible SNP pattern within the QTL on chromosome 13 (Table S1).

A comprehensive analysis of the phenotype-associated SNP variation within the candidate QTLs was also done for the mouse strains for which the complete sequence data are available. Among these strains four represented resistant strains (BALB/cJ, A/J, FVB/NJ and BALB/cOlaHsd), five susceptible strains (LP/J, C3H/HeJ, 129S1/SvImJ, CBA/J and CBA/CaOlaHsd) and four strains with intermediate phenotypes (AKR/J, NOD/ShiLtJ, DBA/2J, and C57BL/6J). In this approach a SNP was classified as phenotype-associated if it was shared exclusively by all the mouse strains representing a given phenotype (i.e. resistant, susceptible or intermediate). Only SNPs differentiating resistant mouse strains from both susceptible and intermediate strains were identified in this analysis. No SNPs were found associated only with susceptible or only with an intermediate phenotype. The resistance phenotype-associated SNPs were located within the intergenic regions and the nine genes (*Ryr1*, *RasGRP4*, *Spint2*, *Ntrk2*, *Stambpl1*, *Acta2*, *Fas*, *Slc16a12* and *Kif20b*) previously identified by EMMA and described above, but phenotype-associated SNPs also were found in a further 13 genes (Table 3). However, these newly identified 13 genes displayed a lower number of phenotype-associated SNPs than the genes identified during the EMMA mapping (Table 3).

The largest number of phenotype-associated SNPs was found within the *Ryr1* gene (over 400), including SNPs causing amino acid change or substitutions within a splicing site (Table 4). The highest number of phenotype-associated amino acid changes was found within the *Map4k1* sequence. There were a further eight genes identified with phenotype-associated amino acid changes (Table 4). The PROVEAN score for each of the detected non-synonymous alterations did not indicate any highly deleterious effect for the tested proteins, with the lowest PROVEAN score of  $-0.87$  and  $-0.74$  for *RasGRP4* and *FAS* respectively (Table 4). Interestingly, the QTL on chromosome 18 was the only one for which the phenotype-associated SNPs were found exclusively within an intergenic region, namely between the *Dcc* and *Smad4* genes. Two more members of the SMAD family were found to be encoded by genes near this QTL: *Smad2* and *Smad7*. An additional SMAD gene, *Smad5*, was found located near the QTL on chromosome 13.

### The pulmonary transcriptome differed between resistant and susceptible mouse strains during pneumococcal infection

Differences in pulmonary gene expression between highly resistant (BALB/cOlaHsd) and highly susceptible (CBA/CaOlaHsd) mouse strains, during the early stage of pneumococcal infection (6 h post-infection), were then investigated. Gene expression was measured using an Illumina MouseWG-6\_V2\_0\_R3 microarray and result submitted to the NCBI Gene

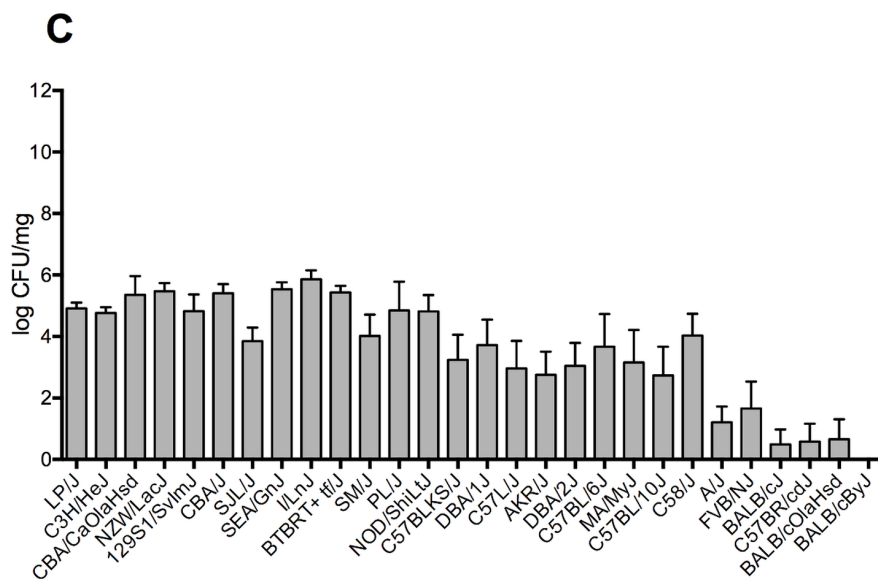
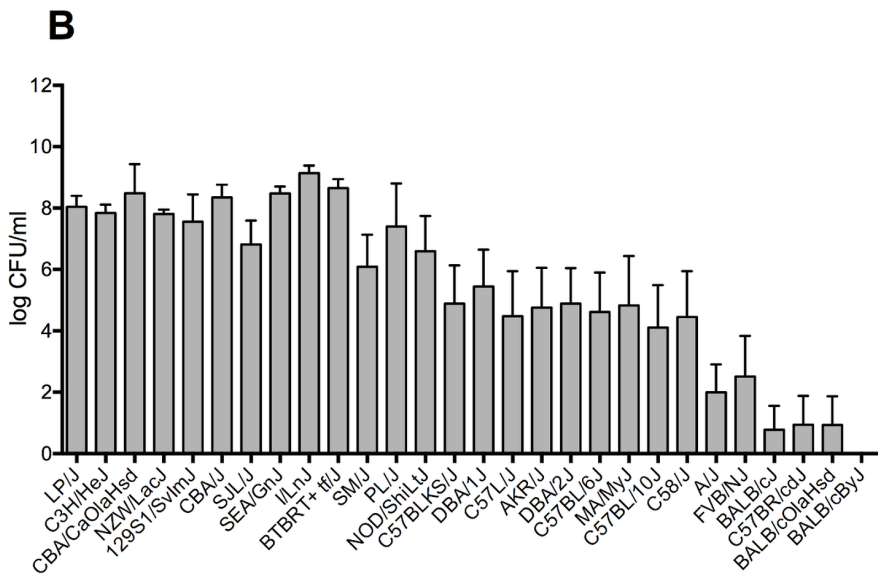
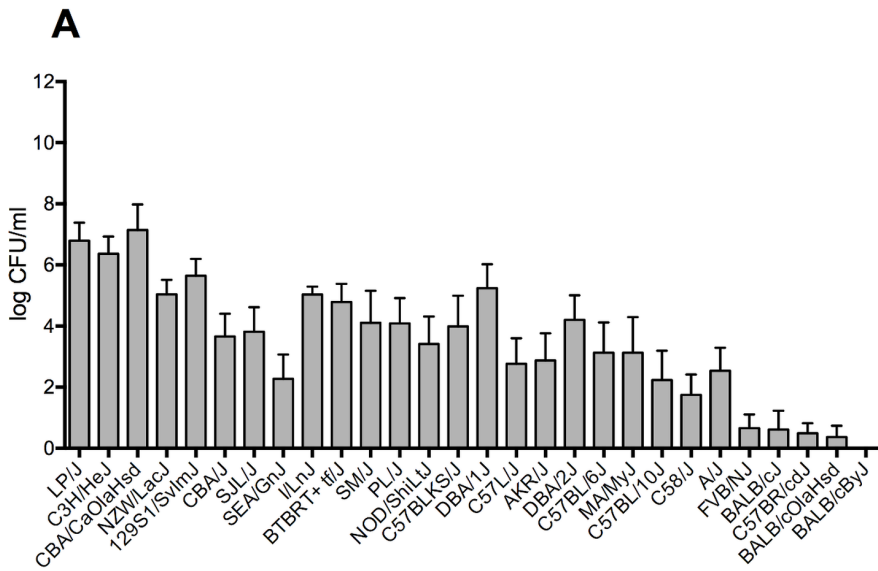


**Figure 1. Bacterial counts in tissues of the tested inbred mice after intranasal-infection with *S. pneumoniae*, D39.** Strains are ordered by increasing mean survival time post-infection. A) Bacterial count in blood 24 h post-infection B) Bacterial count in blood at the time of death C) Bacterial count in lungs at the time of death. Results are for a group of 10 animals. Error bar shows standard error (SE). doi:10.1371/journal.pone.0089831.g001

Expression Omnibus, Accession No: GSE49533. The results were then validated by the real time RT-PCR of 15 selected genes. On average, an 81% correlation was observed between the two methods (Table S2). Genes were considered differentially expressed (DEG) if their expression changed at least 50% compared to sham-infected controls and there was a P value of <0.05. As a result, three lists of DEGs were created: BALB/cOlaHsd infected *versus* control, CBA/CaOlaHsd infected *versus* control and control BALB/cOlaHsd *versus* control CBA/CaOlaHsd. All three lists of DEGs were compared with the list of genes encoded within the QTLs. 30 genes located within the QTLs were differentially expressed in at least at one of the comparisons (Table 5). Five genes with detected phenotype-specific polymorphism were also among the DEGs (*Map4k1*, *Spint2*, *Fas*, *Ppp1r14a* and *Pank1*). Interestingly, *Smad2* located near to the QTL on chromosome 18 was differentially regulated in BALB/cOlaHsd, but not in CBA/CaOlaHsd, during the infection. Two additional members of the SMAD family: *Smad1* and *Smad6* were also differentially expressed during the disease in BALB/cOlaHsd and CBA/CaOlaHsd, respectively (Table 5).

The magnitude of DEGs up-regulation was much higher (about 40-fold change) than that of down-regulation (about 3-fold change) (Fig. 2). Approximately a half of the DEGs were found to be uniquely associated with the infection of only one of the tested mouse strains, either BALB/cOlaHsd or CBA/CaOlaHsd (Fig. 3). Interestingly, though, the magnitude of change of these strain-specific DEGs (uDEGs) was relatively low (up to 4-fold) (Table 6). If the ratio of expression in the two mouse strains of the most highly up-regulated genes (above 4-fold change during infection) was calculated BALB/cOlaHsd and CBA/CaOlaHsd differed at least 2-fold in the regulation of genes encoding leukocytes chemoattractants and protease inhibitors (Table 7).

The DEGs also were analysed with the web-based DAVID tool, in order to identify pathways in which DEGs were over-represented. Consequently, pathways involved in cell proliferation and differentiation (hematopoietic lineage pathway and p53-signalling) and axon guidance signalling were uniquely associated with the pulmonary transcriptome of the resistant BALB/cOlaHsd mice during the infection (Table 8). Interestingly the hematopoietic pathway was also among the most significant pathways when DEGs of control animals (BALB/cOlaHsd *versus* CBA/CaOlaHsd PBS-treated) were compared (Table 8). The pathways unique for susceptible mice were adipocytokine signalling, natural killer cell mediated cytotoxicity, T-cell receptor signalling and cytosolic DNA-sensing pathway (Table 8). Interestingly majority of these pathways are related to immune cell function. Furthermore,

significant enrichment of genes involved in vasculature remodeling and responses to wounding was found in both mouse strains during the infection. The enrichment score for these two clusters was between 8.3 and 10.6, while enrichment scores of any subsequent functional clusters were below 5.5 (Table 9). There was no functional cluster with enrichment score 5 or more for the pulmonary transcriptome of control animals.

### Lung histopathology of BALB/cOlaHsd and CBA/CaOlaHsd mice showed differences in immune cells recruitment

Examination of lung histopathology showed that about 30% of perivascular areas of resistant BALB/cOlaHsd and almost 80% of susceptible CBA/CaOlaHsd mice were affected by cellular infiltration at 24 h post-infection and this difference was statistically significant. However the difference between both mouse strains was not observed at 6 h post-infection when about 30%–40% of perivascular areas of both CBA/CaOlaHsd and BALB/cOlaHsd were affected by cellular infiltrates (Fig. 4). Interestingly, the perivascular areas of resistant BALB/cOlaHsd mice were largely unaffected by immune cells infiltration even though considerable inflammation was present within the lung parenchyma. In contrast, the susceptible CBA/CaOlaHsd mice had substantial accumulation of immune cells within perivascular areas, even when no visible infiltration was observed within alveolar space (Fig. 5).

### Discussion

Pneumococcal infections can lead to a high mortality and morbidity in humans. While substantial effort has been made to understand the pneumococcal attributes that explain this situation, almost nothing has been done to explain the fact that individuals vary in their innate susceptibility to these infections. Identification of the host factors explaining innate resistance or susceptibility would help development of alternative, host-directed therapies and screening tests to identify individuals at risk. In the present study we aimed to identify host factors determining resistance to pneumococcal infection, using mouse models of pneumonia and bacteraemia. We phenotyped a panel of genetically defined inbred mouse strains for their resistance to pneumococcal infection and looked for association between the host genetic background and disease phenotype. Furthermore we analysed differences in gene expression and lung pathology between two mouse strains representing opposite disease phenotypes (susceptible CBA/CaOlaHsd versus resistant BALB/cOlaHsd).

**Table 2. *S. pneumoniae* resistance QTLs identified by genome wide mapping from EMMA and HAM mapping using survival data (h).**

QTL	Chromosome	interval (Mb)	(–)log(Pvalue) EMMA, 4Mil	(–)log(Pvalue) EMMA, 132K	(–)log(Pvalue) HAM
19:34 Mb	19	33.2–36.2	9.8	8.1	6.8
18:73 Mb	18	70.8–74.6	7.9	8.1	6.3
13:59 Mb	13	58–60.3	7.6	8.1	5.2
7:30 Mb	7	28.7–31.3	7.6	7.7	5.1

doi:10.1371/journal.pone.0089831.t002

**Table 3.** Phenotype-specific genetic polymorphisms within *S. pneumoniae* resistance QTLs.

No of SNPs	chrom	gene	consequence	EMMA
>400	7	<i>Ryr1</i>	non-synon, synon, splicing, intron	Y
100–300	19	<i>Stambp1</i>	non-synon, synon, splicing, intron	Y
100–300	19	<i>Slc16a12</i>	non-synon, synon, splicing, intron	Y
100–300	19	<i>Fas</i>	non-synon, synon, intron	Y
100–300	13	<i>Ntrk2</i>	synon, intron	Y
10–100	19	<i>Acta2</i>	synon, intron	Y
10–100	19	<i>Ifit1</i>	non-synon, synon, intron	N
10–100	19	<i>Kif20b</i>	non-synon, synon, splicing, intron	Y
10–100	19	<i>Pank1</i>	synon, intron	N
10–100	7	<i>Kcnk6</i>	synon, intron	N
10–100	7	<i>Catsperg1</i>	synon, intron	N
10–100	7	<i>Map4k1</i>	non-synon, synon, intron	N
10–100	7	<i>Rasgrp4</i>	non-synon, intron	Y
10–100	7	<i>Spint2</i>	intron	Y
>10	13	<i>Agtpbp1</i>	intron	N
>10	7	<i>Yif1b</i>	intron	N
>10	7	<i>IMUP-1</i>	non-synon, intron	N
>10	7	<i>Psm8</i>	synon	N
>10	7	<i>Spred3</i>	intron	N
>10	7	<i>Sipa1</i>	intron	N
>10	7	<i>Ppp1r14a</i>	intron	N

The number of phenotype-associated polymorphisms within the coding region of the QTLs and their consequences. The presented number of SNPs includes the SNPs identified in the EMMA mapping and in the analyses of the full-length sequences within the disease QTLs. No of SNPs – number of phenotype-associated SNPs identified within the gene; Chrom – chromosome, non-synon – SNP causing amino acid change, synon – SNP causing silent mutation, intron – SNP within intron, splicing – SNP within splicing site of the gene. EMMA – indicates whether the genome-wide significant SNPs ( $p$ -value  $< 5 \times 10^{-8}$ ) were identified within the gene during the EMMA mapping: Y=yes, N=no.

doi:10.1371/journal.pone.0089831.t003

**Table 4.** Phenotype-specific genetic polymorphisms within *S. pneumoniae* resistance QTLs leading to amino acid change or alteration within the splicing site.

Gene name	Chrom	Amino acid change			Splicing site	
		SNP_ID	change: R>S	PROVEAN score	SNP_ID or position	nt change: R>S
<i>Map4k1</i>	7	rs31155356	R>C	0.329		
		rs31836292	I>V	-0.328		
		rs31836292	I>V	-0.328		
<i>Ryr1</i>	7	rs51295578	S>A	-0.383	29832579	A>G
					29842146	T>G
					rs48602222	G>A
<i>Stambp1</i>	19	rs30934349	M>I	0.156	rs30754595	C>T
		rs30525805	N>S	0.04		
<i>Slc16a12</i>	19	rs46173389	T>C	-0.011	34749291	C>A
<i>Fas</i>	19	rs30844760	H>R	-0.738		
<i>Ifit1</i>	19	rs50377880	V>I	0.387		
<i>Kif20b</i>	19	rs13483601	E>G	1.586	rs30751713	A>G
<i>Rasgrp4</i>	7	rs45673726	I>M	-0.872		
<i>IMUP-1</i>	7	rs32347251	K>M	2.833		

change: R>S – amino acid or nucleotide change, resistant (R) versus susceptible (S) variant.

doi:10.1371/journal.pone.0089831.t004



**Table 5.** Differentially expressed genes (DEGs) within candidate susceptibility QTL between mice intranasally infected with *S. pneumoniae*, D39 and control animals.

Chrom	QTL	QTL interval (Mb)	Gene name	BALB/c infection	CBA/Ca infection	BALB/CBA controls	BALB/CBA infection
7	7:30 Mb	28.7–31.3	Dmkn	1.6	2.4		–2.4
7	7:30 Mb	28.7–31.3	Ffar2	3.1	4.4		
7	7:30 Mb	28.7–31.3	Fxyd3	1.6		–1.9	
7	7:30 Mb	28.7–31.3	Hcst		1.6	1.6	
7	7:30 Mb	28.7–31.3	Nfkbib	2			
7	7:30 Mb	28.7–31.3	Nfkbid	2.8	3.3		
7	7:30 Mb	28.7–31.3	Ppp1r14a	–1.5			1.8
7	7:30 Mb	28.7–31.3	Tyrobp	1.8	1.8		
7	7:30 Mb	28.7–31.3	Zfp260	–1.5		2.2	1.5
13	13:59 Mb	58–60.3	Isca1		–1.5		
18	18:74 Mb	70.8–74.6	Mbd1	3.1	2.9	–1.9	
19	19:34 Mb	33.2–36.2	Ankrd1	2	1.9	–2.3	–2.5
19	19:34 Mb	33.2–36.2	Ch25h	7.2	5.7	–1.5	–1.7
19	19:34 Mb	33.2–36.2	Fas	2.8	2.3	–1.5	
19	19:34 Mb	33.2–36.2	Ifit3		–1.5	–1.6	–1.6
19	19:34 Mb	33.2–36.2	Pank1	–1.8	–1.6	–2.5	
7	7:30 Mb	28.7–31.3	Capns1			–1.9	
7	7:30 Mb	28.7–31.3	Cd22			5.9	5.2
7	7:30 Mb	28.7–31.3	Cox7a1			2	
7	7:30 Mb	28.7–31.3	Lsr			–2.2	
7	7:30 Mb	28.7–31.3	Map4k1			1.8	
7	7:30 Mb	28.7–31.3	Mrps12			–2.9	–3.2
7	7:30 Mb	28.7–31.3	Psmc8			–10.5	–8.1
7	7:30 Mb	28.7–31.3	Spint2			–1.6	
7	7:30 Mb	28.7–31.3	Zbtb32			2.6	3.1
7	7:30 Mb	28.7–31.3	Zfp27			–2.4	–2
7	7:30 Mb	28.7–31.3	Zfp30			2.5	2.5
7	7:30 Mb	28.7–31.3	Rasgrp4				–2.5
7	7:30 Mb	28.7–31.3	Hspb6				–1.6
7	7:30 Mb	28.7–31.3	Zfp383				–2
13	13:59 Mb	58–60.3	Ubqln1			–1.9	
18	18:74 Mb	70.8–74.6	Elac1			2.2	2.1
18	18:74 Mb	70.8–74.6	Me2			–3	–2.2
18	18:74 Mb	70.8–74.6	Smad2	–1.5		–1.8	–3
8	N/A	N/A	Smad1	1.8			
9	N/A	N/A	Smad6		–1.8		

Pulmonary gene expression 6 h post-infection is represented as fold change between infected and non-infected animals (BALB/c infection: BALB/c-infected versus PBS-treated, CBA/Ca infection: CBA/Ca infected versus PBS-treated), between PBS-treated control animals (BALB/CBA: BALB/c versus CBA/Ca PBS-treated) and between infected BALB/c and infected CBA/Ca (BALB/CBA infection). Chrom. - chromosome.

doi:10.1371/journal.pone.0089831.t005

The tested panel of inbred mouse strains displayed variable disease phenotypes, ranging from death to complete resistance. The time that animal survived the infection (survival) was used to map pneumococcal pneumonia susceptibility/resistance loci and four candidate QTLs on chromosomes 7, 13, 18 and 19 were identified. It is noteworthy that the candidate QTL on chromosome 7 is located within the *S. pneumoniae* resistance QTL 1 (*Spir1*), identified by our previous linkage analysis of BALB/cOlaHsd (refer thereafter as BALB/c) and CBA/CaOlaHsd crosses (refer thereafter as CBA/Ca) [23]. Subsequently, the GWAS mapping

helped to narrow down the *Spir1* locus from 13 Mb to 2.6 Mb. The most statistically significant SNPs identified by EMMA were located within nine genes, or in intergenic regions, and were able to differentiate the resistant from the susceptible mouse strains, therefore they were regarded as phenotype-specific (or phenotype-associated).

We took advantage of the availability of the full nucleotide sequences of thirteen of the tested inbred strains [35] to search for the genes or intergenic regions, carrying potential causal variants. This approach was possible because within the subset of the

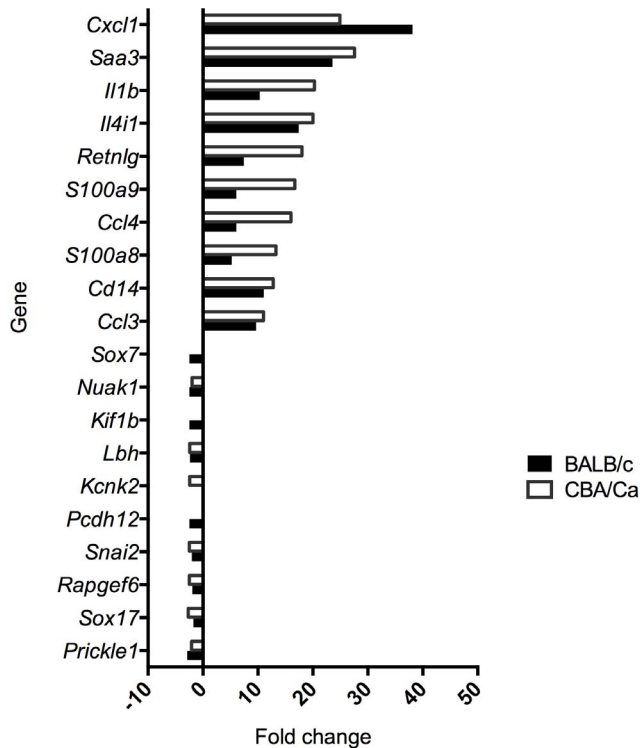


**Figure 2. Change in gene expression 6 h post-infection of BALB/cOlaHsd (resistant) and CBA/CaOlaHsd (susceptible) with *S. pneumoniae*, D39.** Fold change is represented as compared to control animals (PBS-treated). Only the ten most up-regulated and ten most down-regulated genes are presented.  
doi:10.1371/journal.pone.0089831.g002

sequenced inbred strains, the resistant, susceptible and intermediate disease phenotypes were matched in numbers. The analysis resulted in identification of further phenotype-specific SNPs within the nine genes selected by the association analysis, but additionally found thirteen other candidate genes within the QTLs. Among these candidate genes was a member of a solute carrier transporter family: *Slc16a12*. A large number of phenotype-associated SNPs were identified within this gene, some of them leading to a change within the amino acid sequence and the splicing site. This is worth mentioning because one of the best-known genetic factors influencing susceptibility to bacterial infection is a solute carrier transporter, *Slc11a1* (also known as *Nrampl*) [36,37]. The *Slc11a1* gene was not associated with pneumococcal disease in our GWAS but finding another member of the same family associated with resistance to pneumococcal infection may suggest a broader role of the solute carrier transporters during bacterial infection. The transporter associated with pneumococcal disease, *Slc16a12*, belongs to the monocarboxylate transporters [38]. Monocarboxylates, such as lactate, pyruvate or ketones, are important elements of several metabolic pathways and therefore their availability to pneumococci could be crucial for bacterial survival and virulence within the host.

However, the susceptibility to complex diseases such as infectious diseases, most likely depends on networks of genes, with additive genetic effects, or on groups of proteins forming interacting networks [24,28]. Indeed, previous reports show that altered genes underlying disease susceptibility were frequently clustered within the same or related pathways [39,40]. Therefore the discovery of multiple candidate genes and QTLs involved in the susceptibility to pneumococcal pneumonia initiated our

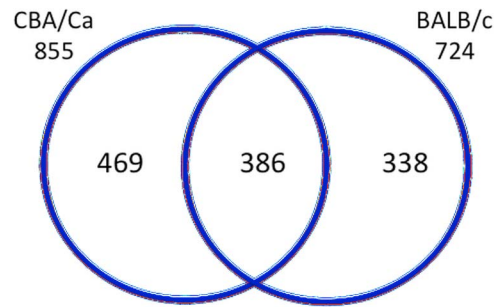


**Figure 3. Number of differentially regulated genes (DEGs) during infection with *S. pneumoniae*, D39.** The included genes show fold change in expression  $\geq 1.5$  and change is significant at  $p \leq 0.05$ . The total number of BALB/cOlaHsd (resistant) and CBA/CaOlaHsd (susceptible) DEGs is indicated below the strain number and amount of commonly and uniquely regulated genes is indicated within the Venn diagram.  
doi:10.1371/journal.pone.0089831.g003

investigation into common aspects of the candidate genes, such as signalling pathways, functional similarities or tissue-specificity.

The presence of a cluster of genes encoding members of the SMAD family within or nearby two of the disease QTLs (*Smad4*, *Smad2* and *Smad7* on chromosome 18 and *Smad5* on chromosome 13) focused our attention on the TGF $\beta$  pathway, in which SMAD proteins are key factors [41,42]. As well as the SMAD genes we

**Table 6. Differentially expressed genes unique (uDEGs) in either BALB/cOlaHsd (resistant) or CBA/CaOlaHsd (susceptible) after intranasal-infection with *S. pneumoniae*, D39.**

uDEG	BALB/c		CBA/Ca	
	FOLD	PVALUE	FOLD	PVALUE
<i>Egr1</i>	4.1	1.00E-04		
<i>Plek</i>	3.0	8.10E-03		
<i>Srgn</i>	3.0	1.90E-03		
<i>Nol5</i>			2.9	4.00E-04
<i>Fos</i>	2.7	1.00E-04		
<i>Ptpn22</i>	2.6	1.00E-04		
<i>Cyp7b1</i>			2.5	1.90E-03
<i>ligp2</i>			2.4	1.40E-03
<i>Abcb1b</i>			2.4	1.60E-03
<i>Igtp</i>			2.3	7.30E-03
<i>Kif1b</i>	-2.0	8.00E-04		
<i>Bcl9l</i>	-2.1	1.00E-04		
<i>Ehd4</i>			-2.1	1.75E-02
<i>Nrp</i>	-2.2	1.36E-02		
<i>Cidec</i>			-2.2	3.60E-03
<i>Gdf10</i>			-2.2	9.00E-04
<i>Krtap17-1</i>			-2.3	3.00E-04
<i>Sox7</i>	-2.4	1.00E-04		
<i>Kif1b</i>	-2.4	1.00E-04		
<i>Kcnk2</i>			-2.4	1.50E-03

Expression is represented as fold change (infected animals versus PBS-treated). Only the five most up-regulated and the five most down-regulated uDEGs are presented for each strain.

doi:10.1371/journal.pone.0089831.t006



**Table 7.** Differentially expressed genes during intranasal-infection with *S. pneumoniae*, D39 in both BALB/cOlaHsd and CBA/CaOlaHsd and showing at least two-fold change difference between the two strains during the infection.

DEG	BALB/c infection	CBA/Ca infection	Fold difference CBA/BALB infected
<i>Serpina3g</i>	2.4	7.7	3.2
<i>Serpina3f</i>	3.1	9.8	3.1
<i>S100a9</i>	6.0	16.7	2.8
<i>Ccl4</i>	6.0	16.0	2.6
<i>S100a8</i>	5.2	13.3	2.6
<i>Retnlg</i>	7.4	18.0	2.4
<i>Fcgr2b</i>	2.7	5.4	2.0
<i>Il1b</i>	10.3	20.3	2.0
<i>F13a1</i>	2.4	4.7	1.9
<i>Cdkn1a</i>	4.1	2.2	-1.9
<i>Fkbp5</i>	5.6	2.7	-2.1

doi:10.1371/journal.pone.0089831.t007

found two other candidate genes with extensive phenotype-specific polymorphism that are associated with the TGF $\beta$  pathway: *Stambpl1* and *Acta2* (both within the QTL on chromosome 19). The former gene encodes the STAM binding protein-like 1 that interacts with SMAD2 and SMAD7 [43] and the later gene

encodes actin smooth muscle, a target gene of TGF $\beta$  signalling [44,45].

Gene expression analysis showed that *Smad2* is significantly down-regulated while *Smad1* and the activin receptor gene *Acvr1b* [43] are up-regulated in the resistant BALB/c mouse during infection, but not in the susceptible CBA/Ca. Interestingly, the

**Table 8.** Significantly regulated pathways (KEGG) during infection and differentiating PBS-treated BALB/c and CBA/Ca mice.

KEGG pathway	BALB/c	CBA/Ca	BALB/CBA control
	PValue	PValue	PValue
Cytokine-cytokine receptor interaction	3.92E-07	2.38E-08	
Pathways in cancer	2.92E-05	6.33E-07	
Toll-like receptor signalling pathway	3.32E-04	1.33E-06	
B cell receptor signalling pathway	3.10E-03	4.43E-05	
Chemokine signalling pathway	9.02E-03	5.10E-05	
MAPK signalling pathway	1.93E-05	1.08E-04	
Apoptosis	1.57E-03	1.09E-04	
Jak-STAT signalling pathway	1.88E-04	3.02E-03	
NOD-like receptor signalling pathway	8.63E-03	5.88E-03	
Hematopoietic cell lineage	1.20E-03		4.30E-04
Axon guidance	3.92E-03		
p53 signalling pathway	4.33E-03		
Adipocytokine signalling pathway		1.56E-04	
Natural killer cell mediated cytotoxicity		9.83E-04	
T cell receptor signalling pathway		6.06E-03	
Cytosolic DNA-sensing pathway		1.05E-02	
Antigen processing and presentation			8.79E-05
Allograft rejection			5.73E-04
Autoimmune thyroid disease			1.10E-03
Graft-versus-host disease			2.16E-03
Type I diabetes mellitus			4.05E-03
Cell adhesion molecules (CAMs)			4.95E-03
Systemic lupus erythematosus			8.53E-03

Names of pathways (KEGG) and their significance (PValue) are provided.

doi:10.1371/journal.pone.0089831.t008

**Table 9.** Functional annotation clustering of differentially expressed genes during pneumococcal infection of BALB/cOlaHsd and CBA/CaOlaHsd.

ID	Description	BALB/c	CBA/Ca
		PValue	PValue
GO:0001944	vasculature development	1.50E-11	3.89E-10
GO:0001568	blood vessel development	3.66E-11	2.04E-10
GO:0048514	blood vessel morphogenesis	5.34E-10	1.78E-09
GO:0001525	angiogenesis	1.79E-08	1.36E-07
<b>Annotation Cluster 1 Enrichment Score:</b>		<b>9.6</b>	<b>8.7</b>
GO:0009611	response to wounding	1.71E-09	1.67E-12
GO:0006954	inflammatory response	1.01E-10	4.72E-12
	inflammatory response	1.06E-08	2.20E-10
GO:0006952	defense response	4.12E-07	2.35E-10
<b>Annotation Cluster 2 Enrichment Score:</b>		<b>8.3</b>	<b>10.6</b>
GO:0042035	regulation of cytokine biosynthetic process		6.54E-07
GO:0042108	positive regulation of cytokine biosynthetic process		2.81E-06
GO:0043123	positive regulation of I-kappaB kinase/NF-kappaB cascade		2.46E-05
<b>Annotation Cluster 3 Enrichment Score:</b>			<b>5.4</b>

Only clusters with enrichment score above 5 are shown. Information provided: the overall enrichment score for the cluster based on EASE score of each member (Enrichment score), name of annotation (Description) and its GO code (ID) if applicable, p-value for the term (PValue).  
doi:10.1371/journal.pone.0089831.t009

*Smad6* and the TGF $\beta$  superfamily receptor *Acvrl1* [46] were significantly down-regulated in susceptible CBA/Ca but not in resistant BALB/c. These observations are in agreement with our previous results that demonstrated an important role of TGF $\beta$  in resistance to pneumococcal infection [21]. We reported significant differences in the concentrations of TGF $\beta$  in BALB/c and CBA/Ca mice and that the higher levels of TGF $\beta$  found in BALB/c lungs during pneumococcal infection correlated with the increase in the number of T regulatory cells (Treg) in the lungs.

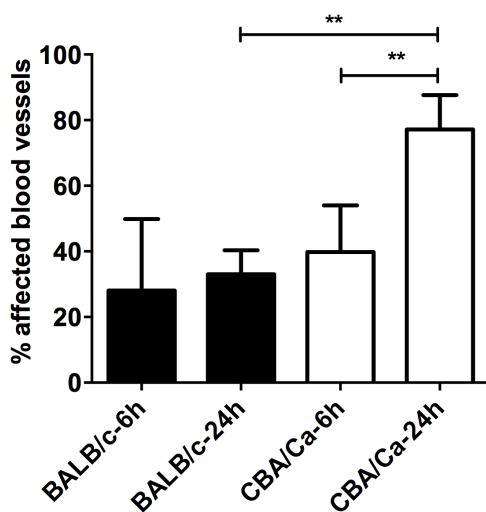


**Figure 4. Percentage of lung's blood vessel affected by inflammation within perivascular areas after infection with *S. pneumoniae* D39.** Results are presented for 6 h and 24 h post-infection for BALB/cOlaHsd (black bars) and CBA/CaOlaHsd (open bars), from two independent experiments, with a total of 5 animals per group. \*\* p<0.001.  
doi:10.1371/journal.pone.0089831.g004

Furthermore we showed that blockade of TGF $\beta$  with a synthetic peptide blocked the induction of Treg cells and decreased BALB/c resistance to infection [21].

In addition to influencing certain immune cells, the TGF $\beta$ -pathway also regulates wound healing, angiogenesis and extracellular matrix production via activation of fibroblast differentiation [44]. The results of our study suggested fibroblast activation and functioning might play a role in the resistance to pneumococcal pneumonia. We demonstrated that the marker of fibroblast activation, *Acta2*, has extensive phenotype-associated polymorphism. Furthermore, we found that during pneumococcal infection the expression of genes known to regulate transcription of *Acta2* differed significantly between resistant and susceptible mice. For example, the candidate gene *Ch25h* encoded within the QTL on chromosome 19 is known to enhance *Acta2* expression and increase TGF $\beta$ 1 release [47]. We showed that transcription of *Ch25h* significantly differed between resistant BALB/c and susceptible CBA/Ca during pneumococcal infection and between control animals. Interestingly, *Ch25h* is located near to the cluster of highly significant intergenic SNPs identified by the EMMA. Therefore it would be interesting to know whether the identified polymorphisms within this intergenic region are responsible for observed differences in *Ch25h* expression. Another example of an *Acta2*-regulating gene was the early growth response factor 1 (*Egr1*), up-regulated only by BALB/c during pneumococcal infection. *Egr1* is known to inhibit TGF $\beta$ -mediated *Acta2* expression [48].

Fibroblasts are ubiquitous cells, which in normal lungs reside in vascular adventitia and airway wall tissue. Beside their vital role in maintaining tissue structure and integrity, fibroblasts also regulate immune cells trafficking, site-specific accumulation and survival [49,50,51]. Furthermore the phenotypic differences between fibroblasts collected from different tissues or even different locations within the organ are widely reported [52,53,54]. One example of such heterogeneity is human pulmonary fibroblasts [49]. It was demonstrated that the

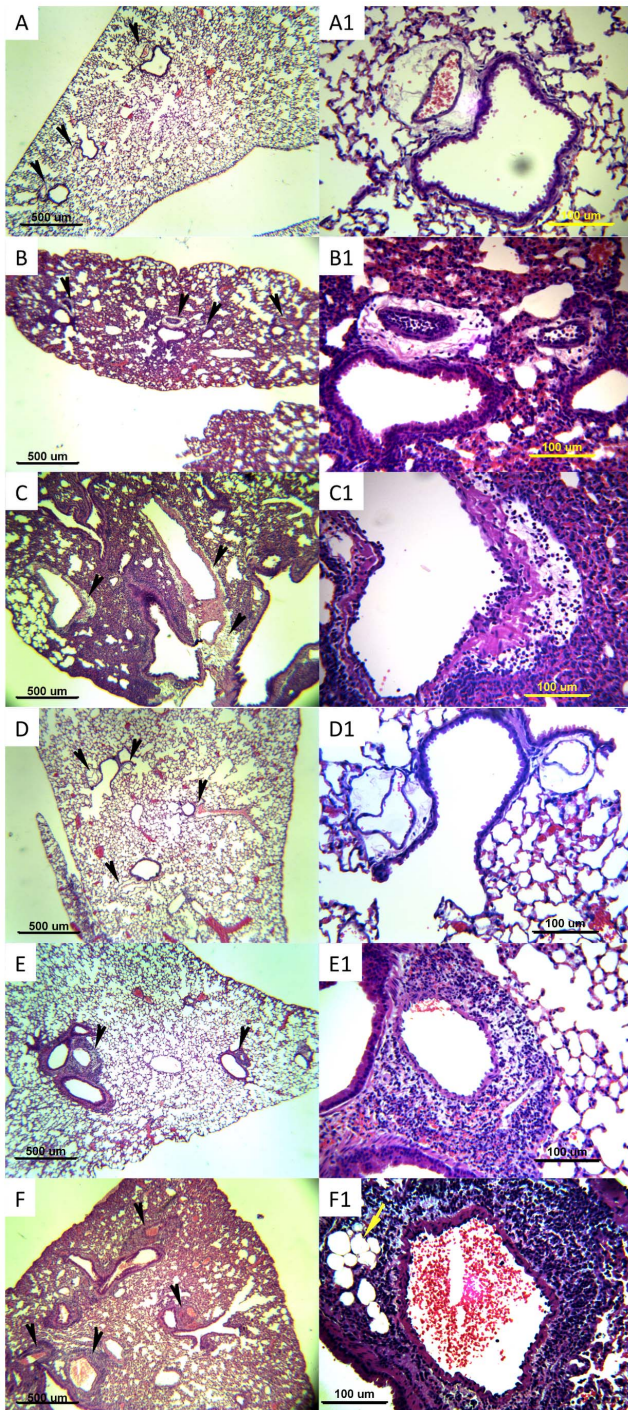


**Figure 5. Inflammation pattern in lungs of BALB/cOlaHsd and CBA/CaOlaHsd mice after infection with *S. pneumoniae*, D39.**

Hematoxylin-and-eosin-stained paraffin wax lung sections from BALB/cOlaHsd (A, A1–C,C1) and CBA/CaOlaHsd (D,D1–F,F1). Panels A,A1 and D,D1 represent lungs of PBS-treated animals, panels B,B1–C,C1 and E,E1–F,F1 are lung sections at 24 h-post infection. Panels A–F represent magnification 40 $\times$  and panels A1–F1 magnification 200 $\times$ . Bar indicates 500  $\mu$ m for 40 $\times$  magnification and 100  $\mu$ m for 200 $\times$  magnification. Black arrows indicate perivascular areas. Yellow arrow in panel F1 indicates perivascular adipose tissue.

doi:10.1371/journal.pone.0089831.g005

fibroblasts residing in the bronchi show higher expression of extracellular matrix (ECM) proteins while the fibroblasts from lung parenchyma display increased TGF $\beta$  signalling and *Acta2* expression. The parenchymal fibroblasts, but not the bronchial ones can rapidly activate endogenous TGF $\beta$  via tension-mediated mechanism [54,55,56]. In the light of the above observations it is particularly interesting to see that the pattern of lung inflammation differs between resistant BALB/c and susceptible CBA/Ca. The cellular infiltrates are located predominantly within lung parenchyma of BALB/c mice while in CBA/Ca it accumulates within peribronchial and perivascular areas [3,9]. Fibroblasts are activated during tissue injury and they can also recognize pathogen-associated molecular patterns (PAMPs) [47]. Rapid activation of TGF $\beta$  by parenchymal fibroblasts could explain observed TGF $\beta$ -mediated increase in Treg population, a feature of BALB/c infection [21]. Considering all the evidence it can be easily envisaged that the differences in the fibroblast phenotypes contributed to the observed differences in the immune cell migration, TGF $\beta$  availability and subsequently to the susceptibility to pneumococcal infection.

The large accumulation of immune cells within perivascular areas of CBA/Ca but not BALB/c mice suggests that the vasculature is involved in the resistance. We showed that perivascular areas of resistant BALB/c mice were either unaffected or mildly inflamed, even when massive inflammation within lung parenchyma was observed. The accumulation of leukocytes within perivascular areas could cause damage to the vessel structure and facilitate bacterial dissemination into the blood, which is a feature of infection of CBA/Ca but not of BALB/c mice. The hypothesis that alteration of the vasculature is a key aspect of susceptibility is further supported by analysis of our pulmonary gene expression data that showed one of the most enriched functional gene clusters during the pneumococcal infection is for the remodelling of lung vasculature. Furthermore, we have found a group of candidate genes with identified phenotype-associated polymorphism to be involved in smooth muscle functioning (*Ryr1*, *Kcnk6*, *Ntrk2*, *Ppp1r14a* and *Kif20b*). *Ryr1* is a calcium channel [57,58], *Kcnk6* is a potassium channel [59], *Ppp1r14a* is a phosphatase inhibitor [60], *Ntrk2* is a neutrophin receptor [61,62] and *Kif20b* encodes a kinesin [63]. The *Ntrk2* knock-out mice show significantly reduced blood vessel formation [64] and *Kcnk6* knock-out mice show vascular dysfunction [59]. Smooth muscles are a product of fibroblast differentiation and an important component of airways and lung vasculature [65,66,67].

Interestingly, we found that the enrichment of genes belonging to the adipocytokine signalling pathway was unique for the CBA/Ca pulmonary transcriptome. This is worth noting because the adipocytokines are secreted predominantly by adipose tissue, which in the lung is located within perivascular areas. This perivascular adipose tissue (PVAT) plays an important role in the regulation of vascular structure and homeostasis [65]. It is known that leukocyte infiltration and their oxygen radical production are key factors in PVAT dysfunction, which in turn leads to compromised blood vessel functionality [68]. Thus the accumulation of immune cells within perivascular areas of CBA/Ca mice is likely to be affecting PVAT functioning. Consistent with this, we observed that the expression of resistin-like molecule  $\gamma$  (*Retnlg*), which is secreted by adipocytes, was almost 3-fold higher in the susceptible CBA/Ca mice during pneumococcal infection.

PVAT is also an important element of a brain-blood vessel axis because nerve endings are present in the PVAT, enabling neuronal control of vessel function [69]. It is therefore of interest that the genes involved in axon guidance were significantly over-represented in the pulmonary transcriptome of infected BALB/c



mice. We also found that the axon guidance receptor gene *Dcc* (netrin receptor *Dcc*) was encoded within the QTL on chromosome 18, in direct proximity of the cluster of highly significant intergenic SNPs. In addition to the axon guidance pathway being involved in the formation of the neuronal network that can control blood vessels and bronchial contractility, it can also regulate leukocyte transmigration from blood to lung tissue [70,71]. This may offer a further explanation to better clearance of immune cells from the perivascular areas of infected BALB/c mice.

It is noteworthy though, that a candidate gene *Ntrk2* (in the QTL on chromosome 13), for a neutrophin receptor, is also involved in cross-talk between nervous and immune systems [72], regulation of Th1/Th2 polarisation [73], T-cells development [74] and smooth muscle cells proliferation [75]. This wide range of *Ntrk2* functions places this gene in a central position linking airway smooth muscle, nervous and immune system, three areas where differences were found between resistant and susceptible strains during pneumococcal infection. In this context it is also notable that *Ntrk2* was recently described as a protecting factor in pneumococcal meningitis [76], making this gene a very promising candidate for further investigation.

There is clear evidence that regulation of immune cell populations differs between resistant and susceptible strains during pneumococcal infection. This can be seen in timing and quantity of cellular infiltrations [3,9], T-cell recruitment [21] and macrophage functioning [77]. Furthermore, the results from our present study showed that pathways that differentiated between pulmonary transcriptomes of resistant and susceptible mice were associated with immune cells proliferation and functioning. We showed that hematopoietic cell lineage and p53-signalling pathways are unique for BALB/c, while pathways involved in immune cells functioning such as T-cells receptor signalling and natural killer cells mediated cytotoxicity were unique to susceptible CBA/Ca mice. Furthermore, we found that candidate genes *Fas*, *Map4k1*, *RasGRP4* and *Spint2* (all but *Fas* encoded within the QTL on chromosome 7) were involved in regulation of immune cells. For example, *RasGRP4* encodes guanine nucleotides exchange factor, which was recently reported to influence ROS production in neutrophils [78] and *Spint2* encodes a Kunitz-type serine protease inhibitor. Interestingly, a Kunitz-type protease inhibitor was reported to suppress pro-inflammatory cytokine production in macrophages and neutrophils [79,80,81] offering possible explanation for observed differences in BALB/c and CBA/Ca macrophages [77]. Two very interesting genes were *Fas* and *Map4k1* both of which showed phenotype-associated amino acid substitutions. Their expression also differed between CBA/Ca and BALB/c in disease or between control animals. Although *Fas* regulates apoptosis in a wide range of cells, *Map4k1* is expressed exclusively in hematopoietic compartment. *Map4k1* plays a pivotal role in regulation of activation induced T-cell apoptosis [82]. This function seems especially interesting because many reports demonstrate that T-cells are recruited and highly engaged during pneumococcal infection [8,21,83] and affect host survival [21,84,85].

The regulation of immune cell populations is a key factor in resistance to pneumococci that can lead to either resolution (associated with resistance) or uncontrolled inflammation (associated with susceptibility). The trafficking of immune cells from the bloodstream to tissues parenchyma is regulated by fibroblasts and may be critical for the host early defences against pneumococci [51]. Furthermore our data demonstrate that lung vasculature may be equally important to host survival, not least because it constitutes an important barrier to bacterial dissemination into blood and development of invasive pneumococcal disease. The

accumulation of immune cells within lung perivascular areas could affect vessel functioning and facilitate bacterial dissemination into blood, a prominent feature of susceptible mice infection. In contrast, migration of leukocytes into lung parenchyma could activate parenchymal fibroblasts and initiate TGF $\beta$ -mediated immunomodulatory responses, a feature of resistant mice infection. This pattern of inflammation is likely a result of inherited differences in lung vasculature (e.g.: fibroblast/smooth muscle cells) and/or immune cells qualities (e.g.: motility or ability to clear bacteria). This is a promising hypothesis since we found that half of the genes carrying phenotype-associated polymorphism have well documented roles in fibroblast differentiation, smooth muscle and immune cells functioning. Therefore we propose that the phenotype of pulmonary fibroblasts may contribute to host survival through regulation of immune cells trafficking, synthesis and activation of TGF $\beta$  and modulation of vessel functioning. Furthermore we speculate that the resistance to pneumococcal infection is modulated by the cumulative effect of alteration within several genetic factors. This hypothesis comes from the discovery of multiple disease QTLs and observation that the phenotype-associated polymorphism was located within very limited number of genes and intergenic regions (22 genes out of few hundred encoded within identified four QTLs). We also observed mixed pattern of susceptible and resistant SNP variants associated with intermediate but not susceptible mouse strains, supporting our speculation on the cumulative effect of candidate genes on resistance to pneumococci.

## Methods

### Ethics statement

All animal experiments were performed in accordance to the UK Home Office guidelines. The University of Leicester Ethics Committee and the UK Home Office approved the study protocols. Animals were housed and experiments carried out at designated facility at the University of Leicester.

### Mice

The female mice of 26 inbred Jax-mouse strains, 10 mice per strain were purchased from The Jackson Laboratory: 129S1/SvImJ, A/J, AKR/J, BALB/cByJ, BALB/cJ, BTBR T+ tf/J, C3H/HeJ, C57BL/J, C57BL/6J, C57BL/10J, C57BLKS/J, C57BR/cdJ, C58/J, CBA/J, DBA/1J, DBA/2J, FVB/NJ, I/LnJ, LP/J, MA/MyJ, NOD/ShiLtJ, NZW/LacJ, PL/J, SEA/GnJ, SJJ/J and SM/J while two strains BALB/cOlaHsd and CBA/CaOlaHsd were purchased from Harlan, UK. Mice were housed in the Division of Biomedical Services, University of Leicester. All mice were fed on fundamental diet. Mice used for the experiments were 9 to 12 week old.

### Bacterial strain

*Streptococcus pneumoniae* serotype 2 strain D39 (NCTC7466) from the National Collection of Type Cultures, Central Public Health Laboratory, London, United Kingdom was used. To prepare a challenge stock bacteria were grown overnight on blood agar base (BAB) plate with 5% horse blood in CO<sub>2</sub> jar at 37°C. Next day bacterial colonies were transferred from the BAB plate to THY media (Gibco) until OD<sub>600</sub> reached 0.2. The primary culture was diluted 100 times in THY and grown at 37°C in anaerobic condition until the culture reached OD<sub>600</sub> corresponding to 1–3 × 10<sup>8</sup> CFU/ml (middle exponential phase). At this point culture was mixed with glycerol (final concentration 10% v/v), aliquot and frozen at –70°C. Culture was stored up to 3 months.

## Infection

To prepare the challenge dose, aliquot of bacteria stock was centrifuged (13 K rpm) and pellet resuspended in PBS to final concentration  $2.5 \times 10^8$  CFU/ml. Mice were lightly anaesthetized with 2.5 to 5.0% (v/v) fluothane (Zeneca Pharmaceuticals, Macclesfield, United Kingdom) over oxygen (1.5 to 2 l/min) and intranasally infected with  $20 \mu\text{l}$  ( $5 \times 10^6$ ) of the challenge dose. 24 h post-infection about  $50 \mu\text{l}$  of blood were taken from the tail vein and bacteria load in blood was measured by viable count (Gingles et al 2001). Mice were closely monitored and the pain score chart was filled every 6 h until animal was lethargic or until the end of the experiment (7 days) when animal was classified as a survivor. This time point was then used as a surrogate for the survival end point. Animals were humanely euthanized by cervical dislocation when they reached the end point, either when lethargic or at the end of the experiment (168 h). At the time of death blood and lung were collected and bacterial load was measured by viable count.

## Phenotype analysis

The time the animal survived the infection (survival), was used for genome-wide associations mapping to identify disease QTLs. Collected data for each mouse were first analysed using statistical software SPSS. Bartlett's test for equal variances was calculated for each mouse strain and phenotype. One-way ANOVA and Tukey's Multiple Comparison post-test were used to check for statistically significant differences between strains. Strains were classified as resistant, sensitive or intermediate based on the ANOVA results of the survival time for each strain. The rate of survival was represented as the percentage of animals that survived the infection (168 h).

## Microarray

Pulmonary gene expression in CBA/CaOlaHsd and BALB/cOlaHsd mice (Harlan, UK) was assessed at 6 h post infection. Mice inoculated with  $20 \mu\text{l}$  of PBS and sacrificed 6 h post-inoculation were treated as control. Six control animals and five infected animals per strain were used in the gene expression experiment. Control and infected mice were sacrificed at 6 h time point and whole lung was removed. Lungs were cut into small squares and immediately immersed in RNAlater (Qiagen). Lung RNA was isolated using RNeasy mini kit (Qiagen) according to manufacturer instructions. cRNA was synthesized using Ambion MessageAmp kit for Illumina arrays according to manufacturer instruction. The whole lung gene expression was done using chip MouseWG-6\_V2\_0\_R3 on Illumina platform. Gene expression data deposited within the NCBI Gene Expression Omnibus (GEO), Accession No: GSE49533.

## Analysis of microarray data

Microarray data were analysed using GenomeStudio (Illumina) and ArrayTrack [86]. Signal intensity data were normalized across all arrays using quantile normalization in GenomeStudio (Illumina) software. The lists of differentially expressed genes were then created using t-test in ArrayTrack. Differentially expressed genes were selected by calculating a ratio between signal intensity of infected and non-infected conditions for each mouse strain or by calculating the ratio between signal intensity of control BALB/cOlaHsd and CBA/CaOlaHsd animals to check for background differences unrelated to infection.

## Real-time PCR

For quantitative RT-PCR, 500 ng of total RNA was reverse transcribed using the RevertAid H Minus First Strand cDNA-

Synthesis Kit according to manufacturer protocol (Fermentas). Real time quantitative PCR was performed in triplicate on a LightCycler 480 Real-Time PCR System (Roche) in a final volume of  $5 \mu\text{l}$  using  $1 \times$  Maxima SYBR Green qPCR master mix (Fermentas) and  $3.3 \mu\text{M}$  of forward and reverse primers for each mRNA tested. Cycling conditions were  $95^\circ\text{C}$  for 15 minutes, and 38 cycles of amplification at  $95^\circ\text{C}$  for 15 seconds,  $60^\circ\text{C}$  for 30 seconds and  $72^\circ\text{C}$  for 30 seconds. Primers were designed to amplify the same transcripts as those tested on the Illumina MouseWG-6\_V2\_0\_R3 whole genome gene expression beadchips (Table S3). Gapdh and Hprt-1 mRNAs were selected for data normalisation using Genorm [87]. The expression of each mRNA tested was normalised to the geometric mean of Gapdh and Hprt-1 expression [87].

## Genome Wide Association Mapping by PLINK

Genotype files (130K SNP panel, Mouse Assembly NCBIM37) for phenotyped inbred Jax-mouse strains were downloaded from Mouse Phenome Database (MPD). To search for haplotype associations (Haplotype Association Mapping, HAM) the mean survival time (hours) was used. Data were analysed using gPLINK version 2.050 [88].

## Genome Wide Association Mapping by EMMA

Measurements for survival in hours for 10 animals per mouse strain were used to search for association using Efficient Mixed Model Association, EMMA [89]. Analyses were done using EMMA Correction Server for all tested inbred mouse strains. EMMA algorithm corrects for population structure and relatedness among inbred mouse strains. QTL mapping by EMMA was done using both 130K and 4Mil SNP panels available.

## QTL selection

The QTLs were considered a candidate disease QTL if at least 3 SNPs within 0.5 Mb were found displaying significance equal or below p-value  $10^{-5}$  for 130K SNP panel and p-value equal or below  $5 \times 10^{-8}$  when 4Mil SNP panel was used. The interval of the QTL was calculated as the region containing significant SNPs with 1 Mb downstream and upstream of this region [90]. The list of candidate QTLs was generated and cross-compared between both methods. QTL that was significant in both EMMA and PLINK was selected as candidate QTL.

## Sequence polymorphism within Harlan BALB/c and CBA/Ca strains within candidate QTLs

For sequencing of BALB/cOlaHsd and CBA/CaOlaHsd mice, DNA was extracted from mouse-tail tissue using the Nucleon kit (Gen-probe). Sequencing was performed at the Wellcome Trust Centre for Human Genetic's High Throughput Genomics Facility (UK), generating 8- to 10-fold coverage of a single lane of PE100 nt per sample on the HiSeq2000. Paired-end Illumina reads from CBA/CaOlaHsd were aligned to the reference genome (C57BL/6J, NCBIM37) using BWA, the same was done for BALB/cOlaHsd. Detection of SNPs in each alignment was made using the Genome Analysis Toolkit (GATK) with default parameters. We adopted a filtering strategy to identify high-confidence SNPs and reduce false positives. SNP sites that failed GATK's internal status check, quality  $<300$  or had an allele ratio  $<0.8$  were removed from any further analysis. Differing SNPs between CBA/CaOlaHsd and BALB/cOlaHsd were then compared to the precompiled SNPs found in 11 strains from the Mouse Genome Project (129S1/SvImJ, A/J, BALB/cJ, C3H/HeJ, CBA/J, FVB/NJ, AKR/J, NOD/ShiLtJ, DBA/2J, C57BL/

6J and LP/J). We generated a list of SNPs between CBA/CaOlaHsd and BALB/cOlaHsd that were copied in CBA/J and BALB/cJ; this was used as the final list of differentiating SNPs. List of SNPs was deposited in NCBI dbSNP [91].

### Gene Identification

Gene list were generated for each selected QTL using MGI Genes and Markers Query Form. Genes within selected QTLs were then compared with the lists of differentially expressed genes during pneumococcal infection of BALB/c and CBA/Ca strains (ArrayTrack). The list of differentially expressed genes between non-disease condition in BALB/cOlaHsd and CBA/CaOlaHsd was also analysed. The sequence of the genes within QTL region was examined using Mouse Phenome Database (MPD) SNP variation query form (NCBIM37). The gene was classified as most likely causal candidate if found within susceptibility QTL and either showed genetic polymorphism within or nearby its coding region or showed change in expression during pneumococcal infection. The identified nucleotide substitutions within candidate genes that led to amino acid change were also analysed using the PROVEAN tool [92] to evaluate an effect of the alteration on the protein function.

### Preparation and analysis of lung tissues sections

At necropsy, tissue samples were immersed in 10% v/v neutral buffered formaldehyde solution prior to conventional processing and embedding in paraffin wax. Histopathological assessment was performed on tissue section stained with haematoxylin and eosin (BDH). Lungs samples were then examined microscopically and vessels with visible perivascular areas were counted as affected (accumulation of cellular influx) or unaffected (clear perivascular areas). The number of affected vessels per lung was then calculated

as a percentage of total number of counted vessels (affected and unaffected) in the lung section. Lungs of five animals per time point (6 h and 24 h) and per mouse strain were examined.

### Supporting Information

**Table S1 The genome-wide significant SNPs (p-value <5×10E-8) identified during the EMMA mapping and their alteration within tested inbred mouse strains.** The SNP ID, Ensemble annotation for the SNP (I – intron variant, U3 – UTR variant 3', Cn – missense, Cs synonymous codon) and log10 p-value scores for the EMMA mapping [GWAS log(p)] are presented. The red colour indicates resistant mouse strain or SNP associated with the resistance to pneumococcal infection. (XLSX)

**Table S2 Correlation between expression scores obtained by microarray and RT-qPCR technique.** (XLSX)

**Table S3 Primer pairs used for RT-qPCR of selected mouse genes.** (XLSX)

### Acknowledgments

We thank Janine E. Moreton for technical assistance with processing of lung sections and Dr. Peter Greaves for his advice on lung pathology.

### Author Contributions

Conceived and designed the experiments: PWA PD MSJ. Performed the experiments: MSJ NS VEF. Analyzed the data: MSJ MS SK AMM PD PWA. Contributed reagents/materials/analysis tools: PWA AMM. Wrote the paper: MSJ PWA PD.

### References

- O'Brien KL, Wolfson LJ, Watt JP, Henkle E, Deloria-Knoll M, et al. (2009) Burden of disease caused by *Streptococcus pneumoniae* in children younger than 5 years: global estimates. *Lancet* 12: 893–902.
- Martens P, Worm SW, Lundgren B, Konradsen HB, Benfield T (2004) Serotype-specific mortality from invasive *Streptococcus pneumoniae* disease revisited. *BMC Infect Dis* 30: 4–21.
- Kerr AR, Irvine JJ, Search JJ, Gingles NA, Kadioglu A, et al. (2002) Role of inflammatory mediators in resistance and susceptibility to pneumococcal infection. *Infect Immun* 70: 1547–57.
- Mizrachi-Nebenzahl Y, Lifshitz S, Teitelbaum R, Novick S, Levi A, et al. (2003) Differential activation of the immune system by virulent *Streptococcus pneumoniae* strains determines recovery or death of the host. *Clin Exp Immunol* 134: 23–31.
- Kadioglu A, Cuppone AM, Trappetti C, List T, Spreafico A, et al. (2011) Sex-based differences in susceptibility to respiratory and systemic pneumococcal disease in mice. *J Infect Dis* 204: 1971–9.
- Marriott HM, Dockrell DH. (2006) *Streptococcus pneumoniae*: the role of apoptosis in host defense and pathogenesis. *Int J Biochem Cell Biol* 38: 1848–54.
- Hollingsworth JW, Whitehead G, Berman KG, Tekippe EM, Gilmour MI, et al. (2007) Genetic basis of murine antibacterial defense to streptococcal lung infection. *Immunogenetics* 59: 713–24.
- Kadioglu A, Gingles NA, Grattan K, Kerr A, Mitchell TJ, et al. (2000) Host cellular immune response to pneumococcal lung infection in mice. *Infect Immun* 68: 492–501.
- Gingles NA, Alexander JE, Kadioglu A, Andrew PW, Kerr A, et al. (2001) Role of genetic resistance in invasive pneumococcal infection: identification and study of susceptibility and resistance in inbred mouse strains. *Infect Immun* 69: 426–34.
- Kadioglu A, Andrew PW (2004) The innate immune response to pneumococcal lung infection: the untold story. *Trends Immunol* 25: 143–9.
- Cruse G, Fernandes VE, de Salort J, Pankhania D, Marinas MS, et al. (2010) Human lung mast cells mediate pneumococcal cell death in response to activation by pneumolysin. *J Immunol* 184: 7108–15.
- van Rossum AM, Lysenko ES, Weiser JN (2005) Host and bacterial factors contributing to the clearance of colonization by *Streptococcus pneumoniae* in a murine model. *Infect Immun* 73: 7718–26.
- Brueggemann AB, Griffiths DT, Meats E, Peto T, Crook DW, et al. (2003) Clonal relationships between invasive and carriage *Streptococcus pneumoniae* and serotype- and clone-specific differences in invasive disease potential. *J Infect Dis* 187: 1424–32.
- Fernebo J, Blomberg C, Morfeldt E, Wolf-Watz H, Normark S, et al. (2008) The influence of in vitro fitness defects on pneumococcal ability to colonize and to cause invasive disease. *BMC Microbiol* 8: 65.
- Blomberg C, Dagerhamn J, Dahlberg S, Browall S, Fernebo J, et al. (2009) Pattern of accessory regions and invasive disease potential in *Streptococcus pneumoniae*. *J Infect Dis* 199: 1032–42.
- Chapman SJ, Khor CC, Vannberg FO, Rautanen A, Walley A, et al. (2010) Common NFKBIL2 polymorphisms and susceptibility to pneumococcal disease: a genetic association study. *Crit Care* 14(6): R227.
- Chapman SJ, Khor CC, Vannberg FO, Rautanen A, Segal S, et al. (2010) NFKBIZ polymorphisms and susceptibility to pneumococcal disease in European and African populations. *Genes Immun* 11: 319–25.
- Chapman SJ, Khor CC, Vannberg FO, Frodsham A, Walley A, et al. (2007) IkappaB genetic polymorphisms and invasive pneumococcal disease. *Am J Respir Crit Care Med* 176: 181–7.
- Glavan BJ, Holden TD, Goss CH, Black RA, Neff MJ, et al. (2011) Genetic variation in the FAS gene and associations with acute lung injury. *Am J Respir Crit Care Med* 183: 356–63.
- Lingappa JR, Dumitrescu L, Zimmer SM, Lynfield R, McNicholl JM, et al. (2011) Identifying host genetic risk factors in the context of public health surveillance for invasive pneumococcal disease. *PLoS One* 6(8): e23413.
- Neill DR, Fernandes VE, Wisby L, Haynes AR, Ferreira DM, et al. (2012) T regulatory cells control susceptibility to invasive pneumococcal pneumonia in mice. *PLoS Pathog* 8(4): e1002660.
- Sun K, Gan Y, Metzger DW (2011) Analysis of murine genetic predisposition to pneumococcal infection reveals a critical role of alveolar macrophages in maintaining the sterility of the lower respiratory tract. *Infect Immun* 79: 1842–7.
- Denny P, Hopes E, Gingles N, Broman KW, McPheat W, et al. (2003) A major locus conferring susceptibility to infection by *Streptococcus pneumoniae* in mice. *Mamm Genome* 14: 448–53.
- Flint J, Eskin E (2012) Genome-wide association studies in mice. *Nat Rev Genet* 13: 807–17.
- Kathiresan S, Musunuru K, Orho-Melander M (2008) Defining the spectrum of alleles that contribute to blood lipid concentrations in humans. *Curr Opin Lipidol* 19: 122–7.



26. Hirschhorn JN, Daly MJ. (2005) Genome-wide association studies for common diseases and complex traits. *Nat Rev Genet* 6: 95–108.
27. Hunter KW, Crawford NP (2008) The future of mouse QTL mapping to diagnose disease in mice in the age of whole-genome association studies. *Annu Rev Genet* 42: 131–41.
28. Flint J, Valdar W, Shifman S, Mott R (2005) Strategies for mapping and cloning quantitative trait genes in rodents. *Nat Rev Genet* 6: 271–86.
29. Liu P, Vikis H, Lu Y, Wang D, You M (2007) Large-scale in silico mapping of complex quantitative traits in inbred mice. *PLoS One* 2(7): e651.
30. Bennett BJ, Farber CR, Orozco L, Kang HM, Ghazalpour A, et al. (2010) A high-resolution association mapping panel for the dissection of complex traits in mice. *Genome Res* 20: 281–90.
31. Manolio TA, Brooks LD, Collins FS (2008) A HapMap harvest of insights into the genetics of common disease. *J Clin Invest* 118: 1590–605.
32. Flint J (2013) Gwas. *Curr Biol* 23(7): R265–6.
33. Leduc MS, Lyons M, Darvishi K, Walsh K, Sheehan S, et al. (2011) The mouse QTL map helps interpret human genome-wide association studies for HDL cholesterol. *J Lipid Res* 52: 1139–49.
34. Su Z, Leduc MS, Korstanje R, Paigen B (2010) Untangling HDL quantitative trait loci on mouse chromosome 5 and identifying *Scarb1* and *Acads* as the underlying genes. *J Lipid Res* 51: 2706–13.
35. Keane TM, Goodstadt L, Danecek P, White MA, Wong K, et al. (2011) Mouse genomic variation and its effect on phenotypes and gene regulation. *Nature* 477: 289–94.
36. Malo D, Vogan K, Vidal S, Hu J, Cellier M, et al. (1994) Haplotype mapping and sequence analysis of the mouse *Nramp* gene predict susceptibility to infection with intracellular parasites. *Genomics* 23: 51–61.
37. Mackenzie B, Hediger MA (2004) SLC11 family of H<sup>+</sup>-coupled metal-ion transporters NRAMP1 and DMT1. *Pflügers Arch* 447: 571–9.
38. Halestrap AP (2013) The SLC16 gene family - structure, role and regulation in health and disease. *Mol Aspects Med* 34: 337–49.
39. Chapman SJ, Hill AV (2012) Human genetic susceptibility to infectious disease. *Nat Rev Genet* 13: 175–88.
40. Degn SE, Jensenius JC, Thiel S (2011) Disease-causing mutations in genes of the complement system. *Am J Hum Genet* 88: 689–705.
41. Miyazono K, ten Dijke P, Heldin CH (2000) TGF-beta signaling by Smad proteins. *Adv Immunol* 75: 115–57.
42. Heldin CH, Moustakas A (2012) Role of Smads in TGFβ signaling. *Cell Tissue Res* 347: 21–36.
43. Ibarrola N, Kratchmarova I, Nakajima D, Schiemann WP, Moustakas A, et al. (2004) Cloning of a novel signaling molecule, AMSH-2, that potentiates transforming growth factor beta signaling. *BMC Cell Biol* 5: 2.
44. Desmoulière A, Geinoz A, Gabbiani F, Gabbiani G (1993) Transforming growth factor-beta 1 induces alpha-smooth muscle actin expression in granulation tissue myofibroblasts and in quiescent and growing cultured fibroblasts. *J Cell Biol* 122: 103–11.
45. Roy SG, Nozaki Y, Phan SH (2001) Regulation of alpha-smooth muscle actin gene expression in myofibroblast differentiation from rat lung fibroblasts. *Int J Biochem Cell Biol* 33: 723–34.
46. Romano V, Raimondo D, Calvanese L, D'Auria G, Tramontano A, et al. (2012) Toward a better understanding of the interaction between TGF-β family members and their ALK receptors. *J Mol Model* 18: 3617–25.
47. Ichikawa T, Sugiura H, Koarai A, Kikuchi T, Hiramatsu M, et al. (2013) 25-Hydroxycholesterol promotes fibroblast-mediated tissue remodeling through NF-κB dependent pathway. *Exp Cell Res* 319: 1176–86.
48. Liu X, Kelm RJ Jr, Strauch AR (2009) Transforming growth factor beta1-mediated activation of the smooth muscle alpha-actin gene in human pulmonary myofibroblasts is inhibited by tumor necrosis factor-alpha via mitogen-activated protein kinase kinase 1-dependent induction of the Egr-1 transcriptional repressor. *Mol Biol Cell* 20: 2174–85.
49. McGettrick HM, Butler LM, Buckley CD, Rainger GE, Nash GB (2012) Tissue stroma as a regulator of leukocyte recruitment in inflammation. *J Leukoc Biol* 91: 385–400.
50. Parsonage G, Filer AD, Haworth O, Nash GB, Rainger GE, Salmon M, Buckley CD (2005) A stromal address code defined by fibroblasts. *Trends Immunol* 26: 150–6.
51. Behzad AR, Chu F, Walker DC (1996) Fibroblasts are in a position to provide directional information to migrating neutrophils during pneumonia in rabbit lungs. *Microvasc Res* 51: 303–16.
52. Wynn TA (2008) Cellular and molecular mechanisms of fibrosis. *J Pathol* 214: 199–210.
53. Meneghin A, Hogaboam CM (2007) Infectious disease, the innate immune response, and fibrosis. *J Clin Invest* 117: 530–8.
54. Wipff PJ, Rifkin DB, Meister JJ, Hinz B (2007) Myofibroblast contraction activates latent TGF-beta1 from the extracellular matrix. *J Cell Biol* 179: 1311–23.
55. Pechkovsky DV, Hackett TL, An SS, Shaheen F, Murray LA, et al. (2010) Human lung parenchyma but not proximal bronchi produces fibroblasts with enhanced TGF-beta signaling and alpha-SMA expression. *Am J Respir Cell Mol Biol* 43: 641–51.
56. Blobel GC, Schiemann WP, Lodish HF (2000) Role of transforming growth factor beta in human disease. *N Engl J Med* 342: 1350–8.
57. Du W, Stiber JA, Rosenberg PB, Meissner G, Eu JP (2005) Ryanodine receptors in muscarinic receptor-mediated bronchoconstriction. *J Biol Chem* 280: 26287–94.
58. Sanderson MJ, Delmotte P, Bai Y, Perez-Zogbi JF (2008) Regulation of airway smooth muscle cell contractility by Ca<sup>2+</sup> signaling and sensitivity. *Proc Am Thorac Soc* 5: 23–31.
59. Lloyd EE, Crossland RF, Phillips SC, Marrelli SP, Reddy AK, et al. (2011) Disruption of K(2P)6.1 produces vascular dysfunction and hypertension in mice. *Hypertension* 58: 672–8.
60. Pagiatakis C, Gordon JW, Ehyai S, McDermott JC (2012) A novel RhoA/ROCK-CPI-17-MEF2C signaling pathway regulates vascular smooth muscle cell gene expression. *J Biol Chem* 287: 8361–70.
61. Kermani P, Hempstead B (2007) Brain-derived neurotrophic factor: a newly described mediator of angiogenesis. *Trends Cardiovasc Med* 17: 140–3.
62. Kermani P, Rafii D, Jin DK, Whitlock P, Schaffer W, et al. (2005) Neurotrophins promote revascularization by local recruitment of TrkB+ endothelial cells and systemic mobilization of hematopoietic progenitors. *J Clin Invest* 115: 653–63.
63. Mandelkow E, Mandelkow EM (2002) Kinesin motors and disease. *Trends Cell Biol* 12: 585–91.
64. Wagner N, Wagner KD, Theres H, Englert C, Schedl A, et al. (2005) Coronary vessel development requires activation of the TrkB neurotrophin receptor by the Wilms' tumor transcription factor Wt1. *Genes Dev* 19: 2631–42.
65. Miao CY, Li ZY (2012) The role of perivascular adipose tissue in vascular smooth muscle cell growth. *Br J Pharmacol* 165: 643–58.
66. Xia YC, Redhu NS, Moir LM, Koziol-White C, Ammit AJ, et al. (2013) Pro-inflammatory and immunomodulatory functions of airway smooth muscle: emerging concepts. *Pulm Pharmacol Ther* 26: 64–74.
67. Koziol-White CJ, Damera G, Panettieri RA (2011) Targeting airway smooth muscle in airways diseases: an old concept with new twists. *Expert Rev Respir Med* 5: 767–77.
68. Szasz T, Bomfim GF, Webb RC (2013) The influence of perivascular adipose tissue on vascular homeostasis. *Vasc Health Risk Manag* 9: 105–16.
69. Guzik TJ, Marvar PJ, Czesnikiewicz-Guzik M, Korb R (2007) Perivascular adipose tissue as a messenger of the brain-vessel axis: role in vascular inflammation and dysfunction. *J Physiol Pharmacol* 58: 591–610.
70. Mirakaj V, Thix CA, Laucher S, Mielke C, Morote-Garcia JC, et al. (2010) Netrin-1 dampens pulmonary inflammation during acute lung injury. *Am J Respir Crit Care Med* 181: 815–24.
71. Morote-Garcia JC, Napiwotzky D, Köhler D, Rosenberger P (2012) Endothelial Semaphorin 7A promotes neutrophil migration during hypoxia. *Proc Natl Acad Sci U S A* 109: 14146–51.
72. Prakash Y, Thompson MA, Meuchel L, Pabelick CM, Mantilla CB, et al. (2010) Neurotrophins in lung health and disease. *Expert Rev Respir Med* 4: 395–411.
73. Besser M, Wank R (1999) Cutting edge: clonally restricted production of the neurotrophins brain-derived neurotrophic factor and neurotrophin-3 mRNA by human immune cells and Th1/Th2-polarized expression of their receptors. *J Immunol* 162: 6303–6.
74. Maroder M, Bellavia D, Meco D, Napolitano M, Stigliano A, et al. (1996) Expression of trkB neurotrophin receptor during T cell development. Role of brain derived neurotrophic factor in immature thymocyte survival. *J Immunol* 157: 2864–72.
75. Kwapiszewska G, Chwalek K, Marsh LM, Wygrecka M, Wilhelm J, et al. (2012) BDNF/TrkB signaling augments smooth muscle cell proliferation in pulmonary hypertension. *Am J Pathol* 181: 2018–29.
76. Li L, Shui QX, Zhao ZY, Zhu XD, Bao WQ (2011) Dynamic changes of TrkB gene expression in *Streptococcus pneumoniae* meningitis after treatment with antibiotics and dexamethasone. *World J Pediatr* 7: 250–6.
77. Ripoll VM, Kadioglu A, Cox R, Hume DA, Denny P (2010) Macrophages from BALB/c and CBA/Ca mice differ in their cellular responses to *Streptococcus pneumoniae*. *J Leukoc Biol* 87: 735–41.
78. Suire S, Lécureuil C, Anderson KE, Damoulakis G, Niewczas I, et al. (2012) GPCR activation of Ras and PI3K in neutrophils depends on PLCβ2/β3 and the RasGEF RasGRP4. *EMBO J* 31: 3118–29.
79. Kanayama S, Yamada Y, Onogi A, Shigetomi H, Ueda S, et al. (2007) Bikunin suppresses expression of pro-inflammatory cytokines induced by lipopolysaccharide in neutrophils. *J Endotoxin Res* 13: 369–76.
80. Wakahara K, Kobayashi H, Yagyu T, Matsuzaki H, Kondo T, et al. (2005) Bikunin suppresses lipopolysaccharide-induced lethality through down-regulation of tumor necrosis factor-α and interleukin-1β in macrophages. *J Infect Dis* 191: 930–8.
81. Matsuzaki H, Kobayashi H, Yagyu T, Wakahara K, Kondo T, et al. (2004) Bikunin inhibits lipopolysaccharide-induced tumor necrosis factor alpha induction in macrophages. *Clin Diagn Lab Immunol* 11: 1140–7.
82. Brenner D, Krammer PH, Arnold R (2008) Concepts of activated T cell death. *Crit Rev Oncol Hematol* 66: 52–64.
83. Kemp K, Bruunsgaard H, Skinhøj P, Pedersen B (2002) Pneumococcal infections in humans are associated with increased apoptosis and trafficking of type 1 cytokine-producing T cells. *Infect Immun* 70: 5019–25.
84. LeMessurier K, Häcker H, Tuomanen E, Redecke V (2010) Inhibition of T cells provides protection against early invasive pneumococcal disease. *Infect Immun* 78: 5287–94.
85. Kadioglu A, Coward W, Colston MJ, Hewitt CR, Andrew PW (2004) CD4-T-lymphocyte interactions with pneumolysin and pneumococci suggest a crucial

- protective role in the host response to pneumococcal infection. *Infect Immun* 72: 2689–97.
86. Tong W, Cao X, Harris S, Sun H, Fang H, et al. (2003) ArrayTrack—supporting toxicogenomic research at the U.S. Food and Drug Administration National Center for Toxicological Research *Environ Health Perspect* 111: 1819–26.
  87. Vandesompele J, De Preter K, Pattyn F, Poppe B, Van Roy N, et al. (2002) Accurate normalization of real-time quantitative RT-PCR data by geometric averaging of multiple internal control genes. *Genome Biol* 3(7): RESEARCH0034.
  88. Purcell S, Neale B, Todd-Brown K, Thomas L, Ferreira MA, et al. (2007) PLINK: a tool set for whole-genome association and population-based linkage analyses. *Am J Hum Genet* 81: 559–75.
  89. Kang HM, Zaiten NA, Wade CM, Kirby A, Heckerman D, et al. (2008) Efficient control of population structure in model organism association mapping. *Genetics* 178: 1709–23.
  90. Kirby A, Kang HM, Wade CM, Cotsapas C, Kostem E, et al. (2010) Fine mapping in 94 inbred mouse strains using a high-density haplotype resource. *Genetics* 185: 1081–95.
  91. Sherry ST, Ward MH, Kholodov M, Baker J, Phan L, Smigielski EM, Sirotkin K (2001) dbSNP: the NCBI database of genetic variation. *Nucleic Acids Res* 29:308–311.
  92. Choi Y, Sims GE, Murphy S, Miller JR, Chan AP (2012) Predicting the Functional Effect of Amino Acid Substitutions and Indels. *PLoS ONE* 7(10): e46688.